

## Epitaxial Thin-Film Deposition and Dielectric Properties of the Perovskite Oxynitride BaTaO<sub>2</sub>N

Young-II Kim,<sup>†</sup> Weidong Si,<sup>‡</sup> Patrick M. Woodward,<sup>\*,†</sup> Eli Sutter,<sup>‡</sup> Sangmoon Park,<sup>§</sup> and Thomas Vogt<sup>§</sup>

Department of Chemistry, The Ohio State University, Columbus, Ohio 43210, Physics Department, Brookhaven National Laboratory, Upton, New York 11973, and USC Nano Center, University of South Carolina, Columbia, South Carolina 29208

Received October 17, 2006. Revised Manuscript Received November 17, 2006

Pulsed-laser deposition was employed to grow epitaxial thin films of the oxynitride perovskite BaTaO<sub>2</sub>N on a conducting SrRuO<sub>3</sub> buffer layer deposited on a 100-cut SrTiO<sub>3</sub> single-crystal substrate. Phase purity and epitaxy were optimized at a substrate temperature of 760 °C in a mixed gas atmosphere of 100 mTorr N<sub>2</sub>/O<sub>2</sub> (~20:1). The dielectric permittivity,  $\kappa$ , of the BaTaO<sub>2</sub>N film was large, exhibiting a slight frequency dependence ranging from about 200 to 240 over the frequency range 1–100 kHz. Furthermore, over the temperature range 4–300 K the permittivity showed minimal variation as a function of temperature. The temperature coefficient of the dielectric constant,  $\tau_\kappa$ , is estimated to be in the range of –50 to –100 ppm/K. The coexistence of high dielectric permittivity and weak temperature dependence is an unusual combination in a single-phase material.

### Introduction

Dielectric materials play an integral role in modern electronic devices. They are employed in capacitors, transducers, actuators, random access memories, and microwave filters.<sup>1–4</sup> Dielectrics can be assessed by figures of merit, the most important of which include dielectric permittivity ( $\kappa$ ), dielectric loss ( $\tan \delta$ ), temperature coefficients of dielectric constant ( $\tau_\kappa$ ) or of resonant frequency ( $\tau_f$ ), and electric field tunability ( $K$ ).<sup>4</sup> Improved device performance can be achieved not only from higher  $\kappa$ , but more importantly from lower values of  $\tau_\kappa$ ,  $\tau_f$ , and/or  $\tan \delta$ . This is particularly true when it comes to the increasingly sophisticated functions that are required by modern devices.<sup>3,5,6</sup>

It would be ideal if a single dielectric material could satisfy all the above criteria simultaneously, but attempts to design such materials are hindered by tradeoffs inherent to the dielectric polarization mechanism itself. Dielectric solids can be broadly divided into two subgroups according to the nature of polarization.<sup>7</sup> Most insulating dielectric materials have

centrosymmetric atomic arrangements and therefore rely on the induced electronic polarization as the primary component of their dielectric response. As a consequence, they tend to exhibit relatively low values of  $\kappa$ , typically  $<50$ . On the plus side, they tend to have fairly low values of  $\tau_\kappa$  and  $\tau_f$  and can be tailored to give low values of  $\tan \delta$ .<sup>8</sup> In contrast, ferroelectric materials have residual dipoles that result from static atomic displacements. This leads to much larger values of  $\kappa$  that can run into the thousands. However, the high- $\kappa$  ferroelectric behavior is invariably accompanied by phase transitions triggered by changes in the crystal structure and ionic polarization mode. As a result,  $\kappa$  is prone to significant and sometimes abrupt changes as a function of temperature. Typically, the dielectric losses are also considerably larger in ferroelectrics.

As described above, the desirable combination of high  $\kappa$  and low  $\tau$  values is rarely found in a single material, but several intriguing exceptions have been reported recently. An extraordinarily high  $\kappa$  of ~80000 was observed in ceramic samples of the centrosymmetric compound CaCu<sub>3</sub>Ti<sub>4</sub>O<sub>12</sub> (space group,  $Im\bar{3}$ ), with a minimal temperature dependence between room temperature and 100 K.<sup>9,10</sup> Epitaxial thin films of CaCu<sub>3</sub>Ti<sub>4</sub>O<sub>12</sub> could also be prepared and characterized with  $\kappa \sim 1500$ .<sup>11</sup> There has been extensive debate in the literature as to the origin of this highly unusual combination of properties. The prevailing sentiment is that the giant dielectric effect in CaCu<sub>3</sub>Ti<sub>4</sub>O<sub>12</sub> is associated with extrinsic microstructural features, such as twin boundaries<sup>12</sup>

\* To whom correspondence should be addressed. Phone: +1-614-688-8274. Fax: +1-614-292-0368. E-mail: woodward@chemistry.ohio-state.edu.

<sup>†</sup> The Ohio State University.

<sup>‡</sup> Brookhaven National Laboratory.

<sup>§</sup> University of South Carolina.

- (1) Davies, P. K.; Roth, R. S. *Chemistry of Electronic Ceramic Materials*; National Institute of Standards and Technology Special Publication 804, 1991.
- (2) Ballato, A. In *Advances in Dielectric Ceramic Materials*; Nair, K. M., Balla, A. S., Eds.; The American Ceramic Society: Westerville, OH, 1998; pp 1–14.
- (3) Reaney, I. M.; Ubic, R. *Int. Ceram.* **2000**, *1*, 43.
- (4) Lines, M. E.; Glass, A. M. *Principles and Applications of Ferroelectrics and Related Materials*; Oxford: New York, 1997.
- (5) Reaney, I. M.; Wise, P.; Ubic, R.; Breeze, J.; Alford, N. M.; Iddles, D.; Cannell, D.; Price, T. *Philos. Mag. A* **2001**, *81*, 501.
- (6) Colla, E. L.; Reaney, I. M.; Setter, N. *J. Appl. Phys.* **1993**, *74*, 3414.
- (7) Rao, C. N. R.; Gopalakrishnan, J. *New Directions in Solid State Chemistry*; Cambridge University Press: Cambridge, 1997; pp 383–387.

- (8) Shannon, R. D. *J. Appl. Phys.* **1993**, *73*, 348.
- (9) Subramanian, M. A.; Dong, L.; Duan, N.; Reisner, B. A.; Sleight, A. W. *J. Solid State Chem.* **2000**, *151*, 323.
- (10) Homes, C. C.; Vogt, T.; Shapiro, S. M.; Wakimoto, S.; Ramirez, A. P. *Science* **2001**, *293*, 673.
- (11) Si, W.; Cruz, E. M.; Johnson, P. D.; Barnes, P. W.; Woodward, P. M.; Ramirez, A. P. *Appl. Phys. Lett.* **2002**, *81*, 2056.

or a barrier-layer capacitor effect originating from the presence of semiconducting grains separated by insulating grain boundaries.<sup>13</sup>

Another intriguing group of materials consists of the ATaO<sub>2</sub>N (A = Ba, Sr, Ca) oxynitride perovskites.<sup>14,15</sup> These phases are the oxynitride equivalents of the extensively studied titanate perovskites, which include the prototypical ferroelectric BaTiO<sub>3</sub> and the intriguing incipient quantum ferroelectrics SrTiO<sub>3</sub><sup>16</sup> and CaTiO<sub>3</sub>.<sup>17</sup> Recently, ceramic samples of BaTaO<sub>2</sub>N and SrTaO<sub>2</sub>N were reported to possess large dielectric permittivities of ~5000 and ~3000, respectively, while at the same time adopting centrosymmetric crystal structures and exhibiting fairly weak temperature dependences (over the temperature range 180–300 K).<sup>15</sup> A possible explanation for this seemingly contradictory combination of properties is that extrinsic effects, such as the internal barrier-layer capacitor mechanism, are responsible for the high dielectric permittivity. However, the electrical characteristics of the bulk and grain boundary components were reported to be inconsistent with the barrier capacitor model.<sup>15</sup>

An alternative explanation is that local deviations from the centrosymmetric cubic structure are responsible for the high permittivity, but the disordered anion distribution prevents the occurrence of cooperative phase transitions. Support for this hypothesis comes from a recent extended X-ray absorption fine structure (EXAFS) spectroscopy study of BaTaO<sub>2</sub>N, which showed that the local Ta<sup>5+</sup> environment is clearly distorted from the perfect octahedral environment of the average crystal structure.<sup>18</sup> Complicating matters is the fact that the relatively high porosity of the ceramic samples (~55% of theoretical density) is less than ideal for assessing the intrinsic dielectric properties. Unfortunately, given the refractory nature of these materials as well as the rather restrictive synthetic conditions needed to maintain the ideal anion stoichiometry, all attempts to obtain highly sintered ceramic or single-crystal samples have been unsuccessful. Thin-film deposition provides an attractive alternate route to a dense, highly crystalline sample. Although no previous reports exist for BaTaO<sub>2</sub>N films, deposition of LaTiO<sub>2</sub>N films by RF-magnetron sputtering has been reported.<sup>19–21</sup>

In this work, we report the preparation of BaTaO<sub>2</sub>N thin films, using pulsed-laser deposition (PLD) techniques,<sup>22</sup> and the characterization of these films. The results provide additional insight into the dielectric properties of this compound. This study also provides an opportunity to explore the influence of heteroepitaxial constraints imposed by the substrate on the unit cell dimensions, the crystal symmetry, and potentially the dielectric properties of BaTaO<sub>2</sub>N. Such effects have been exploited to produce a number of interesting results in recent experimental and theoretical studies on thin-film perovskite oxides.<sup>23–26</sup>

## Experimental Section

A BaTaO<sub>2</sub>N target was obtained by hot-isostatic pressing (American Isostatic Press, Columbus, OH) of a BaTaO<sub>2</sub>N powder sample. A stainless steel can containing the sample powder was evacuated and subjected to the hot-isostatic pressing cycle of 1250 °C for 4 h under 30 kpsi. The polycrystalline BaTaO<sub>2</sub>N powder used to prepare the target was synthesized by heating a mixture of BaCO<sub>3</sub> and Ta<sub>2</sub>O<sub>5</sub> at 1000 °C in a flowing NH<sub>3</sub> atmosphere.<sup>15</sup> BaTaO<sub>2</sub>N thin films were grown by pulsed-laser deposition (PLD) on a 100-cut crystal of SrTiO<sub>3</sub>. To carry out electrical measurements, films were deposited onto a SrRuO<sub>3</sub> buffer layer that had been epitaxially deposited on a SrTiO<sub>3</sub> substrate in situ by PLD prior to growing the BaTaO<sub>2</sub>N film. For all of the PLD experiments, a KrF excimer laser ( $\lambda = 248$  nm) was used with an energy density of ~2.0 J/cm<sup>2</sup> and a repetition rate of 5 Hz. During the deposition of SrRuO<sub>3</sub> onto SrTiO<sub>3</sub>, the substrate temperature was set to 800 °C and an O<sub>2</sub> pressure of 100 mTorr was maintained.

In order to obtain phase-pure samples of the desired perovskite phase, the chamber atmosphere was found to be critical. Initially, the O<sub>2</sub> partial pressure was kept as low as possible since oxide ions have a greater reactivity than nitride ions at the deposition temperature. However, deposition under nominally pure N<sub>2</sub> atmospheres tended to produce conducting films rather than the intended insulating dielectric films. The conductivity is thought to come, at least in part, from the formation of a conducting TaN impurity phase, which was observed in X-ray diffraction (XRD) measurements. To avoid the formation of nitride phases, oxygen was introduced into the PLD chamber during deposition. The partial pressures of both N<sub>2</sub> and O<sub>2</sub> were controlled using two separate mass-flow controllers. It was found that single-phase perovskite films could be deposited when the N<sub>2</sub>/O<sub>2</sub> ratio was ~20:1 and the total pressure was 100 mTorr. The optimal substrate temperature for deposition on SrRuO<sub>3</sub>/SrTiO<sub>3</sub> was also explored, and it was found to be 760 °C. After deposition, the films were cooled to room temperature, by shutting down the power supply to the heater, in ~1 atm of N<sub>2</sub>.

The lattice parameters and growth orientation of the BaTaO<sub>2</sub>N films were examined by X-ray diffraction (XRD) measurements

- (12) Subramanian, M. A.; Sleight, A. W. *Solid State Sci.* **2002**, *4*, 347.  
 (13) Adams, T. B.; Sinclair, D. C.; West, A. R. *Adv. Mater.* **2002**, *14*, 1321.  
 (14) (a) Pors, F.; Marchand, R.; Laurent, Y.; Bacher, P.; Roult, G. *Mater. Res. Bull.* **1988**, *23*, 1447. (b) Gouin, X.; Marchand, R.; Laurent, Y.; Gervais, F. *Solid State Commun.* **1995**, *93*, 857.  
 (15) Kim, Y.-I.; Woodward, P. M.; Baba-Kishi, K. Z.; Tai, C. W. *Chem. Mater.* **2004**, *16*, 1267.  
 (16) Muller, K. A.; Burkard, H. *Phys. Rev. B* **1979**, *19*, 3593.  
 (17) Lemanov, V. V.; Sotnikov, A.; Smirnova, E. P.; Weihnacht, M.; Kunze, R. *Solid State Commun.* **1999**, *110*, 611.  
 (18) Ravel, B.; Kim, Y.-I.; Woodward, P. M.; Fang, C. M. *Phys. Rev. B* **2006**, *73*, 184121.  
 (19) Le Gendre, L.; Le Paven, C.; Pinel, J.; Fassel, D.; Carru, J. C.; Tessier, F.; Marchand, R. *Silicates Industriels* **2004**, *69*, 165.  
 (20) Fassel, D.; Carru, J. C.; Le Gendre, L.; Le Paven, C.; Pinel, J.; Chevire, F.; Tessier, F.; Marchand, R. *J. Eur. Ceram. Soc.* **2005**, *25*, 2085.  
 (21) Le Paven-Thivet, C.; Le Gendre, L.; Le Castrec, J.; Chevire, F.; Tessier, F.; Pinel, J. *Prog. Solid State Chem.*, in press.

- (22) Lowndes, D. H.; Geohegan, D. B.; Puzos, A. A.; Norton, D. P.; Rouleau, C. M. *Science* **1996**, *273*, 898.  
 (23) Choi, K. J.; Bieganski, M.; Li, Y. L.; Sharan, A.; Schubert, J.; Uecker, R.; Reiche, P.; Chen, Y. B.; Pan, X. Q.; Gopalan, V.; Chen, L. Q.; Scholm, D. G.; Eom, C. B. *Science* **2004**, *306*, 1005.  
 (24) Wang, J.; Neaton, J. B.; Zheng, H.; Nagarajan, V.; Ogale, S. B.; Liu, B.; Viehland, D.; Vaithyanathan, V.; Schlom, D. G.; Waghmare, U. V.; Spaldin, N. A.; Rabe, K. M.; Wuttig, M.; Ramesh, R. *Science* **2003**, *299*, 1719.  
 (25) Haeni, J. H.; Irvin, P.; Chang, W.; Uecker, R.; Reiche, P.; Li, Y. L.; Choudhury, S.; Tian, W.; Hawley, M. E.; Craigo, B.; Tagantsev, A. K.; Pan, X. Q.; Streiffer, S. K.; Chen, L. Q.; Kirchoefer, S. W.; Levy, J.; Schlom, D. G. *Nature* **2004**, *430*, 758.  
 (26) Ederer, C.; Spaldin, N. A. *Phys. Rev. Lett.* **2005**, *95*, 257601.

in  $\theta-2\theta$  and also in  $\phi$ -scan modes. For the  $\theta-2\theta$  scan, a Bruker D8 powder diffractometer with the Cu  $K\alpha_1$  radiation (40 kV and 50 mA) was used with an incident Ge 111 monochromator and a Braun position-sensitive detector. The  $\phi$ -scan measurement was conducted using a Philips X'Pert three-circle diffractometer with point-focused Cu  $K\alpha_1/K\alpha_2$  radiation (45 kV and 40 mA) and an incident beam lens to provide parallel optics. Cross-sectional transmission electron microscopy (XTEM)<sup>27</sup> was performed to characterize the microstructure of the film using a JEOL JEM 3000 microscope operated at 300 kV. XTEM samples were prepared by tripod polishing followed by brief low-angle ion milling, which provides very large electron-transparent sample areas while minimizing preparation-induced structural modifications. Dielectric measurements were conducted in the temperature range of 4–300 K, using a method similar to previous reports.<sup>11</sup> The relative dielectric constant was determined from capacitance values measured using a parallel-plate capacitor structure. A portion of the BaTaO<sub>2</sub>N film was etched by HF acid exposing the bottom SrRuO<sub>3</sub> layer. This enabled the SrRuO<sub>3</sub> layer to serve as an electrode. The other electrode was created by evaporating a small-area gold contact on top of the film with a mask. The ac bias voltage for the electrical measurements was 50 mV.

## Results

In physical depositions such as PLD, lattice matching at the film–substrate interface can propagate upward to influence the stability, density, and the epitaxy of the film. BaTaO<sub>2</sub>N ( $a = 4.113 \text{ \AA}$ )<sup>15</sup> has a relatively good lattice match to one of the most common PLD substrates, MgO ( $a = 4.21 \text{ \AA}$ ),<sup>28</sup> although a small amount of tensile stress is expected due to the  $\sim 2\%$  mismatch in their lattice parameters. Indeed, attempts to grow both polycrystalline and 100-oriented films of BaTaO<sub>2</sub>N on 100-cut MgO substrates were successful. However, for characterization of electrical properties, films need to be prepared on a conducting surface. It is ideal to use a highly conducting substrate, but such materials are not always available in practice. A common alternative is to deposit a conducting buffer layer on the substrate prior to depositing the material of interest. One of the most widely used conducting buffer layer materials is the perovskite SrRuO<sub>3</sub>, which has a pseudo-cubic parameter of  $3.95 \text{ \AA}$ .<sup>29</sup> Methods for depositing SrRuO<sub>3</sub> films onto SrTiO<sub>3</sub> ( $a = 3.905 \text{ \AA}$ )<sup>30</sup> have been previously established in the literature.<sup>31</sup> Compressive stresses will result from the lattice mismatches with both SrRuO<sub>3</sub> and SrTiO<sub>3</sub>. However, the lattice mismatch associated with the BaTaO<sub>2</sub>N/SrTiO<sub>3</sub> interface,  $\sim 5.2\%$ , is larger than that of the BaTaO<sub>2</sub>N/SrRuO<sub>3</sub> interface,  $\sim 4.1\%$ . Not surprisingly, our attempts to deposit BaTaO<sub>2</sub>N directly onto SrTiO<sub>3</sub> substrates resulted in various minor phases and multiple lattice orientations, whereas the epitaxy and phase purity of the films were much improved when deposited on SrRuO<sub>3</sub>. Consequently, a conducting SrRuO<sub>3</sub> buffer layer was found to be preferable to the use of commercially available conducting SrTiO<sub>3</sub>:Nb<sup>5+</sup> substrates.

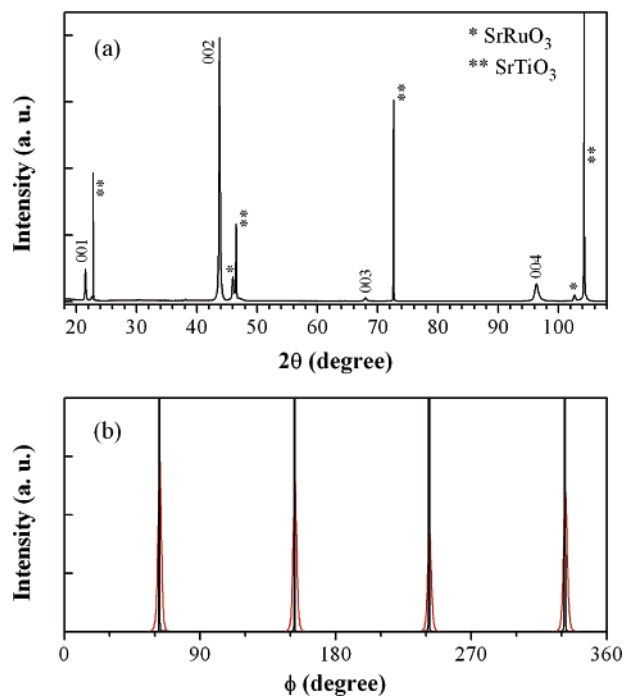


**Figure 1.** XRD patterns of a BaTaO<sub>2</sub>N/SrRuO<sub>3</sub>/SrTiO<sub>3</sub> film measured in (a)  $\theta-2\theta$  scan, and (b)  $110-\phi$ -scan modes (red line: BaTaO<sub>2</sub>N, black line: SrTiO<sub>3</sub>). BaTaO<sub>2</sub>N and SrRuO<sub>3</sub> layers have the thickness of  $\sim 600$  and  $\sim 150$  nm, respectively.

X-ray diffraction measurements in conventional  $\theta-2\theta$  mode were performed on BaTaO<sub>2</sub>N/SrRuO<sub>3</sub>/SrTiO<sub>3</sub> films (Figure 1a). The BaTaO<sub>2</sub>N film as well as the SrRuO<sub>3</sub> buffer layer produced only  $00l$ -type peaks, indicating that the both films were highly oriented with their  $ab$ -planes parallel to that of the SrTiO<sub>3</sub> single-crystal substrate. Using a three-circle diffractometer, additional diffraction peaks could be measured from the BaTaO<sub>2</sub>N film with Bragg indices of  $101$  ( $d = 2.91 \text{ \AA}$ ) and  $112$  ( $d = 1.68 \text{ \AA}$ ). A least-squares refinement using the  $2\theta$  values of the six observed diffraction peaks of the BaTaO<sub>2</sub>N film reveals that the cell dimensions are tetragonally distorted from the cubic symmetry of the bulk phase, with  $a = 4.096(4) \text{ \AA}$  and  $c = 4.1324(7) \text{ \AA}$  ( $c/a = 1.009$ ). Despite the reduction in symmetry, it should be noted that the tetragonally distorted cell has a unit cell volume,  $69.3 \text{ \AA}^3$ , similar to the cell volume of bulk samples with cubic symmetry,  $69.6 \text{ \AA}^3$ .<sup>15</sup> Such a volume-conserving  $ab$ -contraction is consistent with the aforementioned compressive lattice mismatch with the SrRuO<sub>3</sub> underlayer.

An XRD  $\phi$ -scan, with  $\omega$  fixed at the  $[110]$  diffraction condition, was collected to probe the in-plane alignment of the BaTaO<sub>2</sub>N film. As shown in Figure 1b, both the BaTaO<sub>2</sub>N film and the SrTiO<sub>3</sub> substrate produced four equally spaced peaks corresponding to the  $110$ ,  $\bar{1}\bar{1}0$ ,  $\bar{1}10$ , and  $1\bar{1}0$  reflections. The peaks from both BaTaO<sub>2</sub>N and SrTiO<sub>3</sub> are observed at nearly the same  $\phi$  angles, indicating an epitaxial relationship between the BaTaO<sub>2</sub>N films and the SrTiO<sub>3</sub> substrate. Although not probed directly, epitaxial orientation of the SrRuO<sub>3</sub> buffer layer is implied. The peak widths of the BaTaO<sub>2</sub>N reflections ( $\text{fwhm} = 2.3^\circ$ ) were much larger than those of the SrTiO<sub>3</sub> substrate ( $\text{fwhm} = 0.3^\circ$ ), suggesting that the BaTaO<sub>2</sub>N films have relatively small in-plane domains ( $\sim 45 \text{ \AA}$  as estimated by the Scherrer formula). The presence of small domains in the  $ab$ -plane is likely to

(27) Sutter, E.; Williamson, D. *Appl. Phys. Lett.* **2003**, *83*, 5166.

(28) Taylor, D. *Trans. J. Brit. Ceram. Soc.* **1984**, *83*, 5.

(29) Jones, C. W.; Battle, P. D.; Lightfoot, P.; Harrison, W. T. A. *Acta Cryst.* **1989**, *C45*, 365.

(30) Mitchell, R. H.; Chakhmouradian, A. R.; Woodward, P. M. *Phys. Chem. Miner.* **2000**, *27*, 583.

(31) Eom, C. B.; Cava, R. J.; Fleming, R. M.; Phillips, J. M.; Vandover, R. B.; Marshall, J. H.; Hsu, J. W. P.; Krajewski, J. J.; Peck, W. F. *Science* **1992**, *258*, 1766.



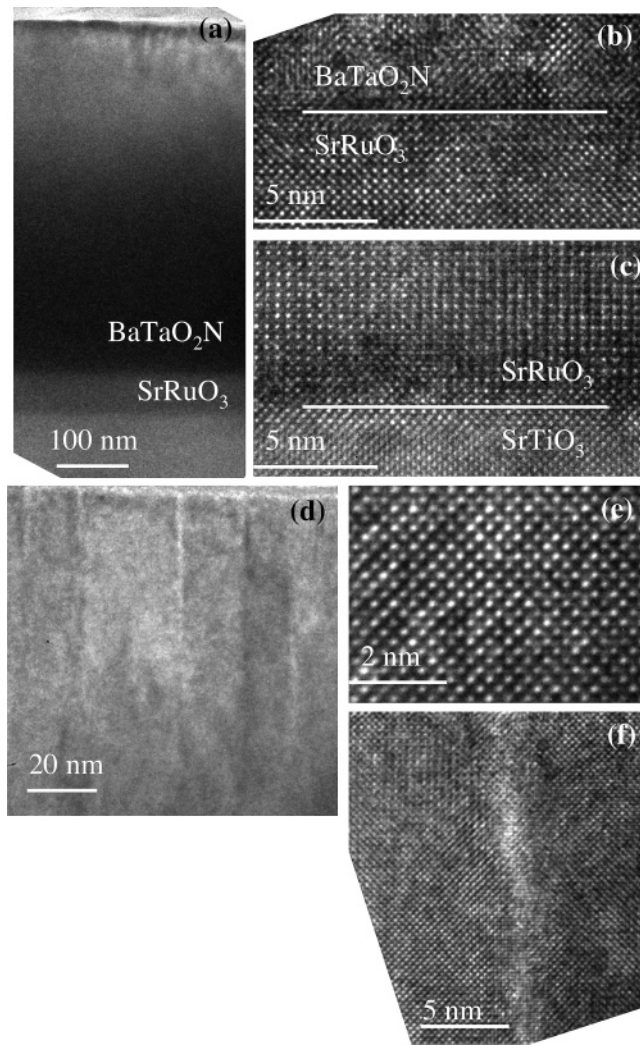


**Figure 2.** XTEM images of a BaTaO<sub>2</sub>N/SrRuO<sub>3</sub>/SrTiO<sub>3</sub> film, (a) low-magnification overview of the cross-section of the film, (b) high-resolution image from the area close to the BaTaO<sub>2</sub>N/SrRuO<sub>3</sub> interface, (c) high-resolution image from the area close to the SrRuO<sub>3</sub>/SrTiO<sub>3</sub> interface, (d) low-magnification image from the BaTaO<sub>2</sub>N layer, (e) high-resolution image of the BaTaO<sub>2</sub>N lattice, and (f) inhomogeneous channel present in the BaTaO<sub>2</sub>N layer.

originate from stress relaxation caused by the BaTaO<sub>2</sub>N/SrRuO<sub>3</sub> lattice mismatch.

The detailed microstructure of BaTaO<sub>2</sub>N/SrRuO<sub>3</sub>/SrTiO<sub>3</sub> film has been investigated by XTEM. In the low-magnification overview image of the film (Figure 2a), the SrRuO<sub>3</sub> and BaTaO<sub>2</sub>N layers can be seen clearly on top of the SrTiO<sub>3</sub> substrate. Details from the BaTaO<sub>2</sub>N/SrRuO<sub>3</sub> and SrRuO<sub>3</sub>/SrTiO<sub>3</sub> interfaces are shown in Figure 2, parts b and c. These figure parts clearly demonstrate that the SrRuO<sub>3</sub> layer is single-crystalline and its interface to the substrate is epitaxial. In the case of the BaTaO<sub>2</sub>N film, initially small grains are formed (Figure 2b) that already have an epitaxial relationship with the underlying SrRuO<sub>3</sub> layer. The small grains quickly coalesce, and a well-formed crystalline structure emerges. A XTEM image showing the morphology of the film away from the BaTaO<sub>2</sub>N/SrRuO<sub>3</sub> interface is shown in Figure 2d. It can be seen that large parts of the film are uniform. However, in some regions, contrast variations are visible. These areas (lines) of lighter contrast on the otherwise uniform film propagate vertically from the SrRuO<sub>3</sub>/BaTaO<sub>2</sub>N

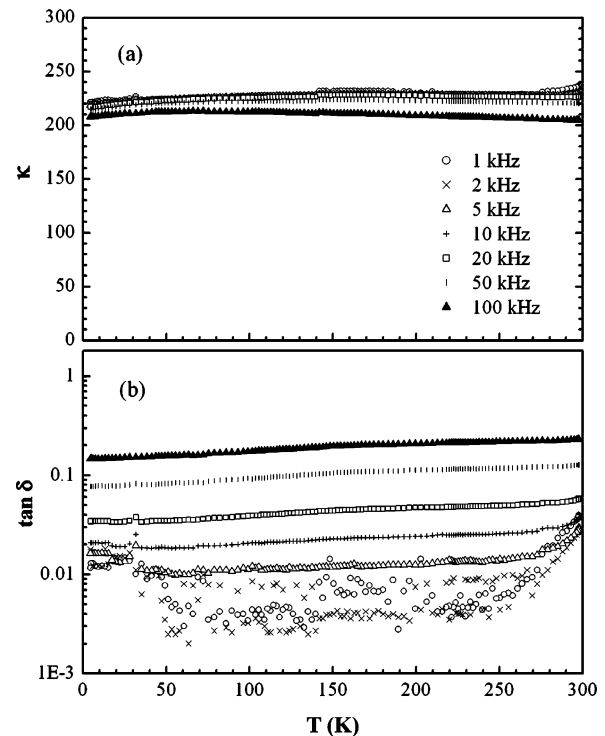


**Figure 3.** Temperature-dependent (a) dielectric permittivity,  $\kappa$ , and (b) dielectric loss  $\tan \delta$  of a 600-nm-thick BaTaO<sub>2</sub>N film. The data legends are the same for both (a) and (b).

interface to the surface of the film. Upon detailed examination, the areas between these lines are seen to be high-quality single-crystalline material (Figure 2f and high-resolution image 2e). The cubic lattice constant of BaTaO<sub>2</sub>N film was estimated as 4.1 Å, in good agreement with the XRD results. Figure 2f shows the area of one of the lighter contrast lines with high resolution. The lattice fringes seem to “traverse” the region of lighter contrast without interruption. Thus, the lighter contrast probably originates from reduced thickness that could be associated with a void channel embedded in the crystalline matrix or an amorphous material at a grain boundary. The nature of those defects was not examined further but the defects appear to be caused by the lattice mismatch between BaTaO<sub>2</sub>N and SrRuO<sub>3</sub> as they are seen to propagate all the way from the interface into the top part of the film.

The dielectric permittivity,  $\kappa$ , and dielectric loss,  $\tan \delta$ , of the BaTaO<sub>2</sub>N film were measured as functions of temperature (4–300 K) and frequency (1–100 kHz), as shown in Figure 3. The dielectric permittivity,  $\kappa$ , of the BaTaO<sub>2</sub>N film ranged from approximately 200 to 240, depending upon frequency, with a negligible temperature dependence. The value of  $\tau_{\kappa}$  is estimated to be in the range of  $-50$  to  $-100$  ppm/K, depending upon the frequency. Compared with the results from incompletely densified BaTaO<sub>2</sub>N ceramic samples,<sup>15</sup> the BaTaO<sub>2</sub>N film possesses a much smaller dielectric permittivity and shows an even smaller temperature dependence.

The dielectric loss of the film also showed a weak dependence on temperature. The loss  $\tan \delta$  at 50 kHz is  $\sim 0.1$ , and it monotonically decreases with the lowering of frequency to fall below 0.01 at 5 kHz. The loss measured for ceramic BaTaO<sub>2</sub>N samples exhibited an opposite frequency

dependence and was larger by more than 1 order of magnitude. It is well-known that microstructure (grain boundaries, etc.), as well as both extended and point defects, can play a dominant role in determining the dielectric loss. As the bulk measurements were carried out on ceramic samples which had attained only  $\sim 55\%$  of their theoretical density,<sup>15</sup> it is perhaps not surprising that the films would show lower losses. It is expected that the losses of BaTaO<sub>2</sub>N films can be lowered significantly if the film growth process can be further optimized. Most significantly, a reduction in the concentration of the defect or void channels revealed in XTEM investigation would be expected to reduce the losses. The most obvious route to reducing such defects is through better lattice matching between the BaTaO<sub>2</sub>N films and the underlying conducting layer. Additionally, a portion of the loss could originate from contact resistance, which was not separated out in the present measurement. The contact resistance is known to be proportional to frequency, which is consistent with the frequency dependence of the loss seen in Figure 3b.

### Discussion

As stated in the introduction, one of the goals of this work was to better characterize and understand the intrinsic dielectric properties of BaTaO<sub>2</sub>N. One of the most obvious results is the observation that the dielectric permittivity for thin-film ( $\kappa \sim 220$ ) and incompletely sintered ceramic ( $\kappa \sim 5000$ ) samples are different by more than an order of magnitude. Which of these values, if either, is more representative of the intrinsic value? While it is difficult to answer that question unequivocally, it is worthwhile to consider the reasons why the two values differ.

The possibility that a boundary-layer capacitor mechanism is responsible for the high permittivity was raised in the introduction. If such a mechanism is responsible for the high permittivity, a reduced concentration in planar defects and grain boundaries (parallel to the substrate) in thin-film samples could explain the reduction of  $\kappa$ . However, as stated in the introduction, the electrical properties of the bulk and grain boundary components in BaTaO<sub>2</sub>N are not consistent with the barrier capacitor model.<sup>15</sup> Furthermore, such a model predicts that the thermally activated intradomain conductivity will cause a Debye-like relaxation behavior in the temperature dependence of loss,<sup>32</sup> but such behavior is not observed in measurements of the thin-film specimen down to 4 K. Therefore, the experimental evidence does not support the boundary-layer capacitor model as a mechanism for explaining the large dielectric permittivity.

How, then, can we explain the difference in the magnitude of  $\kappa$  seen for thin-film and ceramic samples? First, given the high porosity of the ceramic samples, the absolute accuracy of those measurements is somewhat questionable. Therefore, some degree of discrepancy between ceramic and thin-film samples would be expected. Furthermore, it is not unusual for the dielectric permittivity of thin films to be

significantly reduced from values obtained in bulk samples.<sup>11,33,34</sup> Several causes have been called upon to explain the reduced permittivity of thin films, including interfacial dead layer effects<sup>35</sup> and epitaxial strain effects.<sup>36</sup> Given these factors, the true intrinsic dielectric permittivity is likely to be intermediate between the value obtained from thin-film samples ( $\kappa \sim 220$ ) and the value obtained from incompletely sintered ceramic ( $\kappa \sim 5000$ ) samples.

Although the absolute values of the dielectric permittivity for thin-film and ceramic samples differ considerably, there are a number of similarities in their behavior. Both samples possess  $\kappa$  values that are significantly larger than expected for normal insulating solids such as Ta<sub>2</sub>O<sub>5</sub>, SiO<sub>2</sub>, Al<sub>2</sub>O<sub>3</sub>, and so forth.<sup>8</sup> Neither thin-film or bulk samples undergo any structural or electrical phase transitions, which are characteristic signatures of ferroelectrics and relaxors. Furthermore, the temperature dependence of the dielectric permittivity is not characteristic of an incipient ferroelectric, such as SrTiO<sub>3</sub>. In fact, estimates of the  $\tau_\kappa$  values for BaTaO<sub>2</sub>N are both of the opposite sign and much smaller magnitude than even the rutile form of TiO<sub>2</sub>, which has one of the smallest  $\tau_\kappa$  values among incipient ferroelectrics ( $\tau_\kappa = 432$  ppm/K,  $\kappa = 104$ ).<sup>37</sup> This suggests a potentially novel atomistic mechanism for the dielectric behavior of BaTaO<sub>2</sub>N, which merits further study.

The appearance of a tetragonal distortion of the crystal structure induced by epitaxial strain effects is another intriguing result of this study. Because the local Ta–N and Ta–O bonds are not expected to be identical in length, it is possible for the anion distribution to couple with the epitaxial lattice match. While there are no reports of anion ordering in bulk samples of BaTaO<sub>2</sub>N, oxygen/nitrogen ordering has been reported for related phases such as SrTaO<sub>2</sub>N. Günther et al. reported a fully anion-ordered structure for SrTaO<sub>2</sub>N, with nitride ions occupying trans-positions in each Ta-centered octahedron. This is accompanied by a subtle tetragonal distortion ( $c/a = 0.9978$ ).<sup>38</sup> In contrast, Clarke et al. found the oxygen and nitrogen atoms to be almost completely disordered in the same compound.<sup>39</sup> Interestingly, a tetragonal distortion ( $c/a = 1.0016$ ), presumably driven by rotations of the octahedra, was observed despite the general lack of anion order. The discrepancies between these two reports may arise due to differences in synthetic route.

First principles density functional theory calculations on perfectly ordered BaTaO<sub>2</sub>N structures predict that oxygen/nitrogen ordering, with nitride ions occupying trans-positions in each Ta-centered octahedron, would lead to a tetragonal distortion of the unit cell with  $a = 4.06$  Å and  $c = 4.22$  Å

(32) He, L.; Neaton, J. B.; Cohen, M. H.; Vanderbilt, D.; Homes, C. C. *Phys. Rev. B* **2002**, *65*, 214112.

(33) Bai, G. R.; Streiffer, S. K.; Baumann, P. K.; Auciello, O.; Ghosh, K.; Stemmer, S.; Munkholm, A.; Thompson, C.; Rao, R. A.; Eom, C. B. *Appl. Phys. Lett.* **2000**, *76*, 3106.

(34) Suzuki, K.; Kijima, K. *Vacuum* **2006**, *80*, 519.

(35) Zhou, C.; News, D. M. *J. Appl. Phys.* **1997**, *82*, 3081.

(36) Li, H. C.; Si, W.; West, A. D.; Xi, X. X. *Appl. Phys. Lett.* **1998**, *73*, 190.

(37) Wakino, K.; Minai, K.; Tamura, H. *J. Am. Ceram. Soc.* **1984**, *67*, 278.

(38) Günther, E.; Hagenmayer, R.; Jansen, M. *Z. Anorg. Allg. Chem.* **2000**, *626*, 1519.

(39) Clarke, S. J.; Hardstone, K. A.; Michie, C. W.; Rosseinsky, M. J. *Chem. Mater.* **2002**, *14*, 2664.

( $c/a = 1.039$ , volume =  $69.6 \text{ \AA}^3$ ).<sup>40</sup> This distortion is much larger than those reported for bulk samples of SrTaO<sub>2</sub>N, which raises some questions regarding assignment of complete anion order in SrTaO<sub>2</sub>N.<sup>38</sup> Calculations on an ordered structure where the nitride ions occupy the cis-positions of each Ta-centered octahedron give a structure where the  $a$  and  $b$  axes expand while the  $c$ -axis contracts ( $c/a = 0.9879$ ).<sup>40</sup> It is interesting to compare these predictions with the tetragonal distortion observed in this study for BaTaO<sub>2</sub>N films:  $a = 4.10 \text{ \AA}$  and  $c = 4.13 \text{ \AA}$  ( $c/a = 1.009$ , volume =  $69.3 \text{ \AA}^3$ ). While the agreement between observation and experiment is not perfect, the  $c/a$  ratio deviates from unity in a direction that would seem to favor trans-ordering of the nitrogen atoms so that the N–Ta–N–Ta– chains are oriented perpendicular to the substrate. The possibility that the anion-ordering characteristics can be controlled, or at least impacted, by tailoring the epitaxial lattice match with the underlying layer is an intriguing and unexplored research direction.

### Conclusion

An epitaxial structure of BaTaO<sub>2</sub>N/SrRuO<sub>3</sub>/SrTiO<sub>3</sub> was successfully grown by pulsed-laser deposition at a substrate

(40) Fang, C. M.; de Wijs, G. A.; Orhan, E.; de With, G.; de Groot, R. A.; Hintzen, H. T.; Marchand, R. *J. Phys. Chem. Solids* **2003**, *64*, 281.

temperature of 760 °C in a mixed gas atmosphere of 100 mTorr N<sub>2</sub>/O<sub>2</sub> (~20:1). Epitaxial strain effects lead to a tetragonal distortion of the BaTaO<sub>2</sub>N perovskite unit cell, with negligible volume change. Over the temperature range 4–300 K, BaTaO<sub>2</sub>N films exhibit dielectric permittivities,  $\kappa$  of 200 ~ 240, depending upon frequency (1–100 kHz), and  $\tau_\kappa$  of –50 ~ –100 ppm/K. This unique combination of high- $\kappa$  and insensitivity to changes in temperature is not characteristic of any well-known class of dielectric materials. Furthermore, this combination is attractive for a number of device applications. Further studies, with various substrates and buffer layer materials, are needed fully to investigate the influence of lattice matching and stresses on the structure, anion-ordering characteristics, and dielectric properties of BaTaO<sub>2</sub>N.

**Acknowledgment.** This work was supported by the Department of Energy under Contract No. DE-AC02-98CH10886 (Proposal 5229) and the National Science Foundation through the Center for the Design of Materials (CHE-043567). P.M.W. also acknowledges the Sloan Foundation for support as an Alfred P. Sloan Research Fellow. The  $\phi$ -scan XRD measurement was obtained with the help of Prof. Paul Salvador at Carnegie Mellon University.

CM062480K